The hydrothermal diamond-anvil cell - a tool to study trace element behavior in various hydrothermal systems up to 800°C and 1 GPa

M. Borchert, A. Ehnes, I. Schwark, A. Watenphul and K. Appel

Deutsches Elektronen-Synchrotron, Notkestr. 85, 22607 Hamburg, Germany

Hydrothermal diamond-anvil cells (HDAC) are designed to study in-situ (trace) element behavior in fluids at elevated pressures and temperatures by X-ray spectroscopic methods. Therefore, this type of DAC is a great tool to investigate geo-relevant processes including aqueous fluids, e.g., mineral solubilities, element partitioning and element speciations in various systems [1–9].

So far, no HDAC was available from the infrastructure for extreme conditions research at PETRA III. The conceptual in-house design is based on a modified Bassett-type cell [1,3,5,10] and should fulfil the following requirements: I) small size, II) easy handling, and III) fast assembly in order to offer the HDAC also to the user community and to use it at various beamlines (e.g., L, P06, P02.2). General beamline requirements are I) a spot size $\leq$ 20 μm (small sample volume), II) a long focal distance of at least 50 mm, and III) a high photon flux. Furthermore, chemical analysis of elements with Z$\leq$20 is impossible due to the high absorption of the fluorescence signal of these elements in the diamonds. In Fig. 1 different stages of the cell development are presented: technical drawings (A – C), close-up views of the HDAC proto-type (D – F), and a top view image of the cell at beamline L during first test measurements (G). The cell design allows to collect the fluorescence signal in the optimal geometry, i.e. in 90° to the incoming x-ray beam in the plane of polarisation due to a recess in the lower diamond anvil. This recess represents the effective fluorescence detection volume. The HDAC is designed to enable experiments at maximum temperatures and pressures of 800°C and ~1 GPa. Therefore, the cell is resistively heated at both anvils and double-side temperature measurements are performed using K-type thermocouples attached to the diamond anvils. Power supplies for the the resistive heaters are controlled with Eurotherm®2408 temperature controllers within an accuracy of ±0.5°C. Temperature measurements are calibrated based on the ice melting point, well-known melting points of $K_2Cr_2O_7$ and AgCl as well as on the optical observation of the α-β phase transition of quartz. During heating, the HDAC is water-cooled (see Fig. 1C and 1G) and oxidation of metallic parts and diamonds is prevented by flushing the cell with inert gas (N_2+1%H_2). Pressure is determined using an eligible equation of state, the measured liquid–vapour homogenisation temperature, and the vapour–saturated ice melting temperature of the fluid.

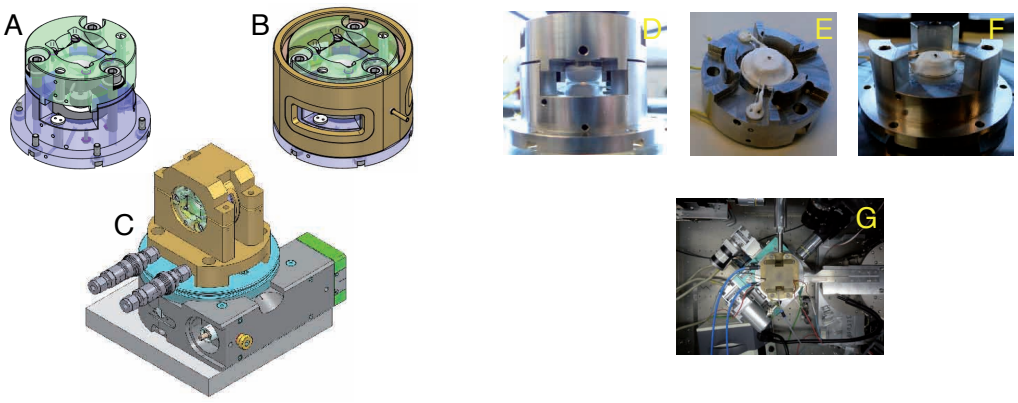

Figure 1: various stages of the HDAC development: from technical drawings (A – C) to the HDAC prototype (D – F) and first test measurements at beamline L (G).

First measurements to test the performance of the HDAC have been done at beamline L (DORIS) in November 2011. The fluorescence signal has been collected using a confocal setup, i.e. a silicon drift detector equipped with a detector capillary as described by [11]. First, a Rb-Sr solution was measured with an excitation energy of 20.3 keV (Fig. 2(a)). The spectrum is compared to data on the same solution collected in 2008 at beamline L using a HDAC from GFZ Potsdam and a detector collimator instead of the confocal arrangement. The experimental setup was also tested at 10 keV in order to determine lower limits of detection

of Cr for future applications. Corresponding XRF spectra are presented in Fig. 2(b). All in all, the in-house designed HDAC passed all tests with success. Loading and alignment of the cell is easy and the quality of the XRF spectra is - so far - absolutely satisfactory. In addition, the first external user group (S. Klemme and co-workers) performed in-situ measurements at beamline L to determine the solubility of apatite in various aqueous fluids already in december 2011.

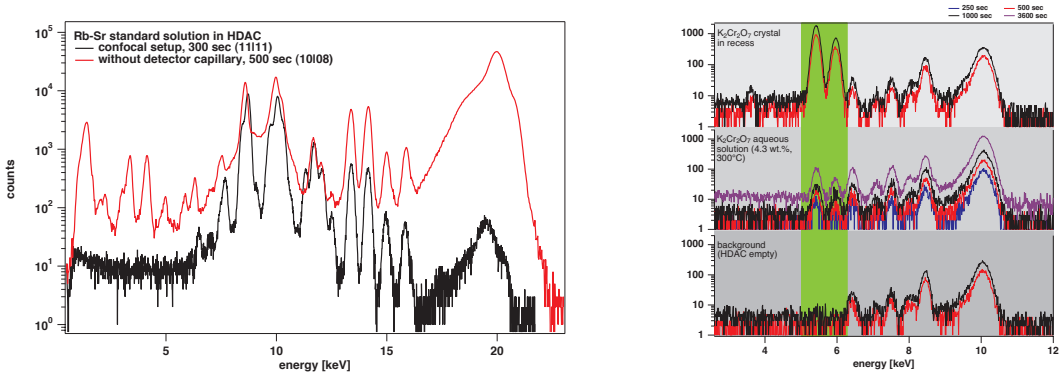

(a) Rb-Sr solution

(b) Cr data

Figure 2: Micro-XRF spectra of a Rb-Sr standard solution measured with and without a detector capillary are shown in Fig. 2(a). Data on Cr in $K_2Cr_2O_7$, solid and dissolved in H_2O, are presented in Fig. 2(b). In addition, measurements in the empty cell were performed in order to determine the background signal from the cell which is negligible in case of Cr.

We like to thank S. Petitgirard (ESRF) and M. Wilke, R. Schulze, C. Schmidt and M. Kreplin from GFZ Potsdam for their help and constructive remarks during all stages of the cell construction!

References

[1] Schmidt, C. and Rickers, K. (2003) *American Mineralogist* **88**, 288–292.

[2] Schmidt, C., Rickers, K., Wirth, R., Nasdala, L., and Hanchar, J. M. (2006) *American Mineralogist* **91**, 1211–1215.

[3] Schmidt, C., Rickers, K., Bilderback, D. H., and Huang, R. (2007) *Lithos* **95**, 87–102.

[4] Bureau, H., Ménez, B., Malavergne, V., Somogyi, A., Simionovici, A., Massare, D., Khodja, H., Daudin, L., Gallien, J.-P., Shaw, C., and Bonnin-Mosbah, M. (2007) *High Pressure Research* **27(2)**, 235–247.

[5] Borchert, M., Wilke, M., Schmidt, C., and Rickers, K. (2009) *Chemical Geology* **259**, 39–47.

[6] Borchert, M., Wilke, M., Schmidt, C., Cauzid, J., and Tucoulou, R. (2010) *Chemical Geology* **276**, 225–240.

[7] Mayanovic, R. A., Anderson, A. J., Bassett, W. A., and Chou, I.-M. (2007) *Chemical Geology* **239**, 266–283.

[8] Mayanovic, R. A., Anderson, A. J., Bassett, W. A., and Chou, I.-M. (2007) *Review of scientific instruments* **78**, 1–9.

[9] Mayanovic, R. A., Anderson, A. J., Bassett, W. A., and Chou, I.-M. (2009) *Chemical Geology* **259**, 30–38.

[10] Bassett, W. A., Shen, A. H., Bucknum, M., and Chou, I.-M. (1993) *Review of scientific instruments* **64**, 2340–2345.

[11] Wilke, M., Appel, K., Vincze, L., Schmidt, C., Borchert, M., and Pascarelli, S. (2010) *Journal of Synchrotron Radiation* **17**, 669–675.